Eur. Phys. J. E (2006)
DOI 10.1140/epje/i2005-10119-2

THE EUROPEAN PHYSICAL JOURNAL E

Frustrated structure of an anticlinic-like smectic-C phase

P.J. Sebastião[1,2,a], P. Simeão Carvalho[3], M.R. Chaves[3], H.T. Nguyen[4], and A.C. Ribeiro[1,2]

[1] Centro de Física da Matéria Condensada, Av. Prof. Gama Pinto 2, 1649-003 Lisboa Codex, Portugal
[2] Instituto Superior Técnico, Departamento de Física, Av. Rovisco Pais, 1049-001 Lisboa Codex, Portugal
[3] Departamento de Física, IFIMUP, Faculdade de Ciências da Universidade do Porto, Rua do Campo Alegre 687, 4169-007 Porto, Portugal
[4] CNRS, Centre de Recherche Paul Pascal, Av. A. Schweitzer, 33600 Pessac, France

Received 1 August 2005 and Received in final form 5 February 2006 /
Published online: 3 May 2006 –

Abstract. We present a polarising optical microscopy study of the low-temperature anticlinic-like tilted mesophase of the liquid-crystal compound octylphenyl-2-chloro-4-(*p*-cyano-benzoyloxy) (DB_8Cl). This mesophase has been described as a bilayer smectic structure in which the molecules within each layer are organised in an anticlinic way. The optical textures observed in samples with planar orientation show a double stripe pattern, with the lines aligned parallel to the rubbing direction, characteristic of a double periodic modulation of the refractive index of the material. The long-period modulation is temperature dependent and disappears for thin sample cells ($< 5\,\mu$m). The short-period modulation is nearly independent of the thickness of the cells. The experimental results are analysed in terms of a model which considers that there is a special distribution of the principal optical axis which may be in or out of the polariser-analyser plane. The observed periodic variation of the principal optical axis could not be interpreted in terms of the original structure proposed for this phase. DB_8Cl presents a structure formed by dimers that can be viewed as flexible bent-core–like molecules, showing similarities with phases found in banana-like systems, but exhibiting a much more complex structure.

PACS. 61.30.-v Liquid crystals – 61.30.Eb Experimental determinations of smectic, nematic, cholesteric, and other structures – 77.84.Nh Liquids, emulsions, and suspensions; liquid crystals

1 Introduction

Polarising optical microscopy (POM) is a powerful technique that can be very helpful in order to understand the molecular structure of liquid crystals (LCs) [1–4]. From the optical textures that can be observed in controlled conditions, it is possible to infer some conclusions with respect to the molecular organisation in mesophases. The results obtained from optical studies are in general complemented by X-ray diffraction studies. With both techniques it is possible, in general, to identify and characterise the structure of mesophases.

Tilted smectic phases are characterised by the smectic layer's spacing and by the molecular tilt angle with respect to the layer's normal. This angle is null for smectic-A phases and has a temperature-dependent value in the smectic-C phases. In the case of ferroelectric phases (SmC*), the direction of the molecular tilt rotates from layer to layer around the normal to the layers and a helical structure is thus formed, with a pitch as a characterising parameter. The optical patterns observed for SmC and SmC*, with a planar alignment of the molecules, are in general different from those observed for SmA phase and quite different from those observed for SmC_A and SmC_A^* phases. In particular, for short pitch ferroelectrics, stripe patterns can be observed in surface stabilised ferroelectric liquid-crystal (SSFLC) cells, which are interpreted as a periodic modulation of the refractive index due to the existence of different smectic domains with different molecular orientations [2]. However, stripe patterns are not exclusive of ferroelectric chiral phases. They have also been observed in smectic-C phases of achiral materials [5] and in the smectic synclinic antiferroelectric (SmC_SP_A) B_2 phase [6] of more complex systems, formed by the so-called banana-like molecules.

It is well known that liquid crystals with strong polar terminal groups, such as the CN group, can present very interesting polymorphisms including monolayer, partial bilayer and bilayer smectic phases [7]. The liquid-crystal compound octylphenyl-2-chloro-4-(*p*-cyano-benzoyloxy), DB_8Cl for short, presents a nematic and three bilayer

[a] e-mail: pedros@lince.cii.fc.ul.pt

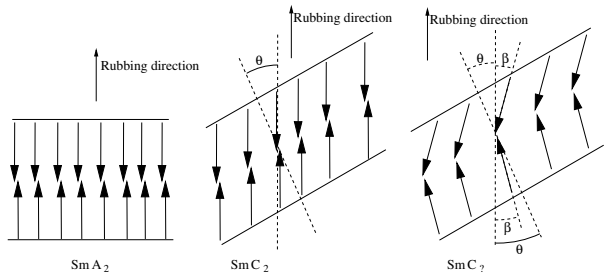

Fig. 1. Schematic representation of the smectic phases of DB_8Cl, as proposed in reference [8].

smectic phases: a smectic-A_2 (SmA_2), a smectic-C_2 (SmC_2) and an anticlinic-like smectic-C phase ($SmC_?$):

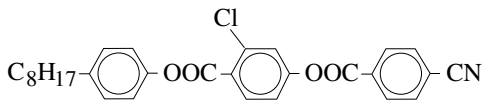

Cr 100°C **SmC?** 107°C **SmC$_2$** 117°C **SmA$_2$** 155°C **N** 168°C **I**

The phase structure of both smectic-A_2 and -C_2 phases is well known and their schematic representation is shown in Figure 1. In this figure, the surface alignment direction in planar cells is identified by the rubbing direction. As for the low-temperature smectic-C_2 phase, an anticlinic-like structure was proposed based on dielectric [8], X-ray diffraction [9] and NMR studies [10]. The structure proposed for the $SmC_?$ phase considers that the molecules in each sublayer present different tilt angles, thus forming a bended dimer, as shown in Figure 1.

The initial proposed structure for the $SmC_?$ phase presents some similarities with an anticlinic phase. The relatively small dielectric response to an electric field parallel to the molecules ($\epsilon_\parallel$) and perpendicular to it ($\epsilon_\perp$) suggests weak polar properties [8], but does not give any indication about the *ferro-* or *antiferro*-electric character of that phase.

In order to understand how the differences between the $SmC_?$ and the SmC_2 phase structures influence the optical textures observed by optical microscopy, we have done some optical studies on DB_8Cl. In Section 2 we present the experimental results concerning this study. In Section 3 we analyse and discuss the results obtained in terms of a new structure model proposed for the $SmC_?$ phase. The main conclusions are outlined in Section 4.

2 Experimental results

The liquid-crystal DB_8Cl was observed between crossed polarisers in a microscope Olympus BHSM using optical objectives of ×25 and ×125 total magnifications. Commercial liquid-crystal cells of 25 μm, 15 μm, 5 μm and 3 μm thickness (EHC Co. Japan), with planar alignment surface treatments, were used in order to understand the influence of the sample's thickness on the observed textures.

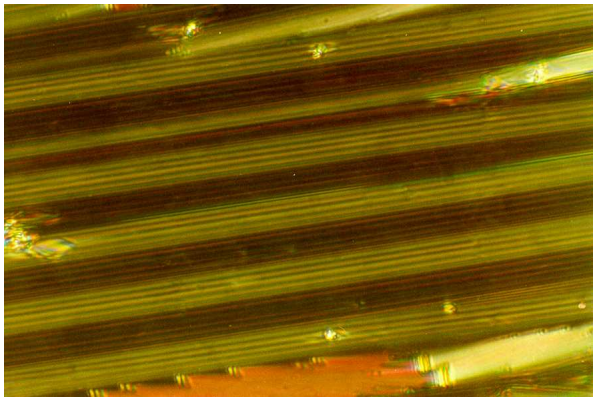

Fig. 2. Texture of the DB_8Cl in a 15 μm cell, in the $SmC_?$ at 98.7 °C rotated −5° with respect to the alignment direction observed between crossed polarisers (×125 magnification).

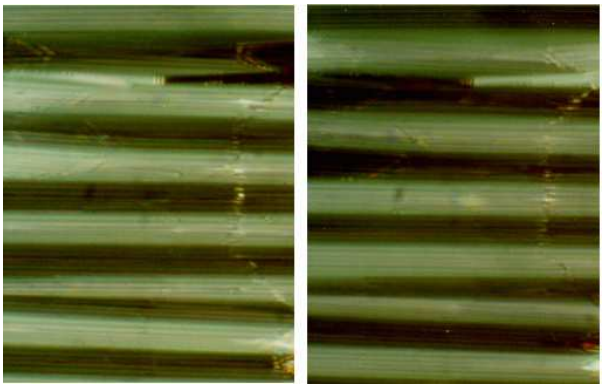

a) b)

Fig. 3. Texture of the DB_8Cl in a 15 μm cell, in the $SmC_?$ at 98.7 °C observed with the crossed polarisers rotated 10° (a) and 80° (b) with respect to the alignment direction (×125 magnification).

Home-made liquid-crystalline preparations using a shearing process as an alignment method were made in order to understand the influence of the surfaces' treatment on the molecular alignment. The samples were put inside a home-made oven, placed in a calibrated rotating stage attached to the microscope, allowing the rotation of the samples perpendicular to the incident light with an accuracy of 0.1°. The temperature of the samples was controlled by a Chromel-Alumel thermocouple with an accuracy better than 0.05 °C.

Before all measurements, the samples were heated up to the isotropic phase of the liquid crystal and then slowly cooled to the desired working temperature to achieve a good molecular alignment.

All textures presented in this work were obtained with a photo camera Olympus OM-4Ti using standard films of 400 ASA processed and printed on standard photo paper. Some pictures were digitalised in order to be numerically treated by computer.

In Figure 2 we present the texture of DB_8Cl, obtained in the $SmC_?$ phase at 98.7 °C with a 15 μm cell, where the rubbing direction makes an angle of 5° with the polariser.

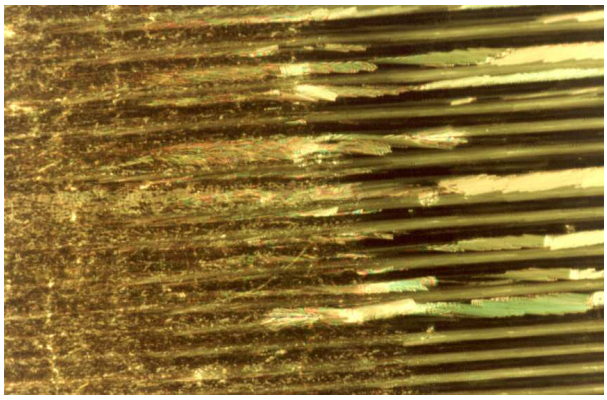

Fig. 4. Texture of the DB_8Cl in a 25 μm cell, under crossed polarisers rotated 6° with respect to the alignment direction, obtained on cooling, during the SmC_2-$SmC_?$ phase transition (×25 magnification).

Two sets of periodic light modulations are observed: one set with a short period of 8 μm (hereafter referred as stripes) and another one with a half-period of $\sim$ 68 μm hereafter referred as a superstructure (dark/light bands). Figures 3a and b show the textures observed for sample rotation angles Δ of 10° and 80°, in the same sense with respect to the polariser, respectively. In these figures it can be observed that the bands change from dark to light (and vice versa) as the sample is rotated.

These textures with bands and stripes were not observed in none of the higher-temperature mesophases of this compound. In Figure 4 we present a photo obtained on cooling DB_8Cl at the SmC_2-$SmC_?$ phase transition. On the photo's left-hand side the sample is still in the SmC_2 phase. On the right side of the photo it can be seen that the pattern of bands and stripes corresponding to the $SmC_?$ is in formation. The texture of the two phases is completely distinct from each other.

The texture of the $SmC_?$ phase is dramatically influenced by the glass cell surface treatment and the samples' thickness. In Figures 5a and b we present textures of two different types of top/bottom glass treatment sets. In Figure 5a, both top and bottom glasses are covered with a conducting film of indium tin oxide (ITO). In Figure 5b neither the top nor the bottom glasses have ITO. In both figures the arrow indicates the shearing direction of the upper glass relatively to the lower one.

As can be observed, the presence of ITO on both glass surfaces (Fig. 5a), without any additional surface treatment that may induce planar alignment, is not enough to promote the superstructure observed in the textures of Figures 2 and 3. The superstructure can be obtained either with commercial cells specially prepared to induce planar alignment of molecules, or by shearing the LC if ITO free substrates are used. In fact, in Figure 5b, where neither surface was coated with ITO, the superstructure is clearly observed, with defect lines nearly parallel to the shearing direction. The immediate conclusion is that the presence of ITO demands a more sophisticated surface treatment

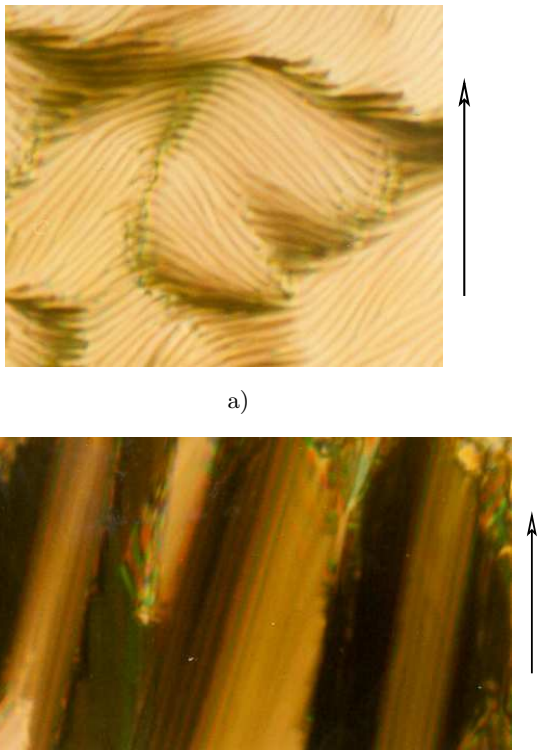

a)

b)

Fig. 5. Texture of the DB_8Cl $SmC_?$ phase at 106.7 °C, observed between crossed polarisers (×125 magnification) in a 15 μm cell, with the crossed polarisers rotated 5° with respect to the shearing direction (represented by the arrow). (a) ITO on top and bottom substrates. (b) Both top and bottom substrates without ITO.

Table 1. Sample's thickness dependence of the bands' half-width, stripes' width and number of observed stripes.

Sample's thickness (μm)	Half-width of bands (superstructure) (μm)	Width of stripes (μm)	Number of stripes per band
25	108.6	8.0	13
15	65.3	8.0	8
5	–	10.2	–
3	–	10.6	–

of the glasses, in order to induce a good planar alignment, which is not obtained by a simple shearing.

In both Figures 5a and b, the short-period stripes are equally spaced. This indicates that the molecular structure responsible for the short-period stripes pattern is weakly dependent of the alignment conditions. Moreover, the width of the stripes increases only slightly with the sample's thickness decrease, as evidenced in Table 1. This result strongly suggests that the short-period light modulation is a characteristic behaviour of the mesophase's structure.

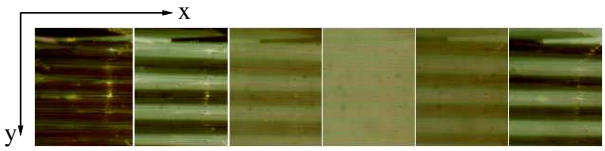

Fig. 6. Textures obtained at different angles Δ between one of the crossed polarisers and the rubbing direction of DB_8Cl, in the $SmC_?$ phase at 98.7 °C. From left to right, the textures refer to angles Δ of 0 °C, 10 °C, 30 °C, 45 °C, 60 °C and 80 °C, respectively. The two directions x and y, referred in the text, correspond to the cell's frame of reference with x parallel to the rubbing direction.

The number of stripes per band decreases strongly with decreasing sample's thickness in the superstructure, while the stripe width remains nearly constant. For the thinner samples (5 μm and 3 μm thickness), no bands could be seen. This behaviour results from the decrease of the bands' width with sample's thickness. In fact, it is interesting to note that the ratio between the sample's thickness, $d_1/d_2 = 25\mu\text{m}/15\mu\text{m} \sim 1.67$, is nearly the same ratio of the corresponding band's width presented in Table 1. If we assume that this ratio is kept for thinner samples, the width of the bands in 5 μm thick samples should be nearly twice the width of the stripes. In such a case, it would be hard to distinguish bands from stripes.

In order to study the dependence of the contrast ratio between the stripes on the angle Δ between the polariser and the rubbing direction, several photos were obtained for angles between 0° and 90°. Figure 6 presents the photos obtained for different angles in a local frame of reference. In this figure, x and y have a direction parallel and perpendicular to the stripes, respectively, with x parallel to the rubbing direction.

As can be observed in Figure 6, for $\Delta \sim 45°$ there is an inversion of the dark/light regions of the superstructure.

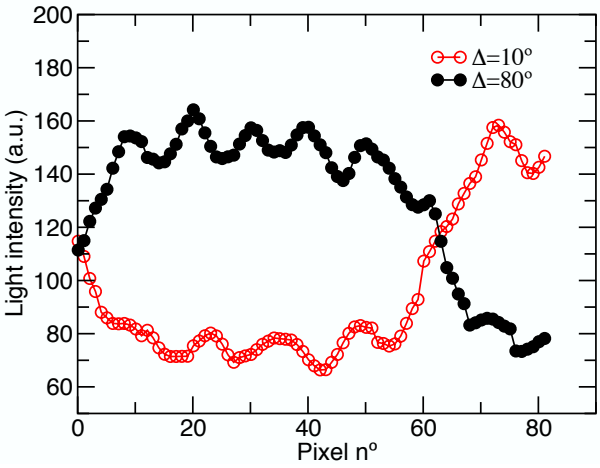

Fig. 7. Experimental averaged transmitted light intensity profile in the y-direction for two orientation angles Δ (10° and 80°) of the cell.

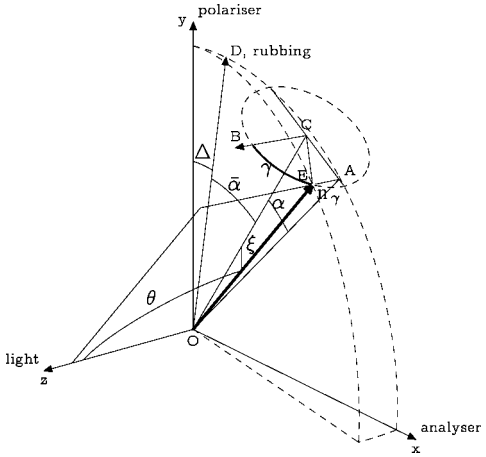

Fig. 8. Frame of reference xyz, illustrating the orientation distribution of the optical axis as described in the text.

3 Analysis and discussion

Stripe patterns have been observed in planar aligned cells of liquid-crystalline compounds [2,5,6]. However, as mentioned before, what is different in the patterns observed with DB_8Cl is the existence of two sets of modulations as depicted in Figure 6. The transmitted light intensity profile in the direction y (perpendicular to the stripes) for two orientation angles Δ of the cell with respect to the polariser ($\Delta = 10°$ and $\Delta = 80°$) is shown in Figure 7. This profile was obtained after converting the colour picture to a grey scale and performing an average over several pixel intensities in the direction x (parallel to the stripes) (see Fig. 6). For the sake of clarity only a small area was covered, corresponding to a size of a few microns.

As can be observed in Figure 7, the light intensity in the pattern has a continuous and periodic modulation in the y-direction, with an average value that changes with y when the band changes from dark to light (or from light to dark) in the superstructure. The light intensity variation between the dark/light bands has an amplitude higher than that of the small modulation observed for the stripes within each band.

In fact, the experimentally observed modulations can be described in the following, considering the frame of reference xyz presented in Figure 8. In that figure, OD is the rubbing direction. The OC direction, making an angle $\bar{\alpha}$ with OD in the polariser-analyser plane (xOy), can be defined. The dark bands have the lowest average intensity when OC is aligned with the polariser (y-axis). For cell orientations of an angle α relatively to $\bar{\alpha}$ the stripes within the dark bands show small light intensity changes. The direction of the optical axis defined at the layer scale by the molecular dimers is represented in Figure 8 by a unit vector $\mathbf{n}_\gamma$, which may be placed *in* or *out* of the xOy-plane. OA is one of the directions of the electric displacement; CB is a direction parallel to the z-axis and γ is the angle defined by CB and CE directions; θ is the angle defined by z and $\mathbf{n}_\gamma$; Δ is an angle defined by y and OD; finally, ξ is the angle between OC and $\mathbf{n}_\gamma$, and α is defined by OC and OA.

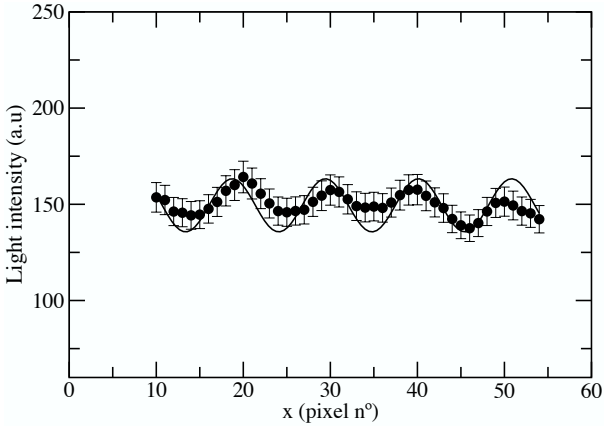

Fig. 9. Transmitted light intensity model fit to the experimental data for the angle $\Delta = 80°$.

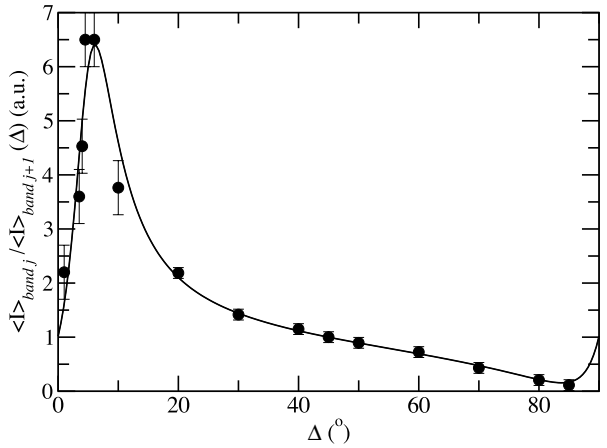

Fig. 10. Model fit using equation (6) to the experimental light intensity ratio.

By using simple trigonometric relations, it can be shown that the angles α, ξ and γ are related by the expression

$$\tan(\alpha) = \tan(\xi)\sin(\gamma). \tag{1}$$

The light intensity resulting from the observation of an uniaxial medium between crossed polarisers obeys the law [11],

$$I = I_0 \sin^2\left(\frac{\delta}{2}\right)\sin^2(2\Omega), \tag{2}$$

where

$$\Omega = \Delta + \bar{\alpha} + \alpha$$

and

$$\delta = \frac{2\pi h}{\lambda}\Delta n \sin^2(\theta) = \frac{2\pi h}{\lambda}\Delta n\left(1 - \sin^2(\xi)\cos^2(\gamma)\right). \tag{3}$$

In these equations, Δn is the optical birefringence, h is the cell's thickness and I_0 is the maximal light intensity. For the sake of simplicity, ξ is considered constant, although in a more general case we may have $\xi(\gamma)$. The spatial distribution of the principal optical axis is obtained by writing γ as a function of y and assuming positive and negative $\bar{\alpha}$ values. In a first approximation we shall consider

$$\gamma = \frac{2\pi}{L}y, \tag{4}$$

where L is the stripes' width. Since we have used white light with a bandwidth spectrum $\Delta\lambda = \lambda_M - \lambda_m$, and no appreciable light dispersion is observed within the resolution of the equipment used, the average light intensity at a certain point y can be obtained by

$$\langle I\rangle_{\Delta\lambda}(y) = \frac{I_0}{\Delta\lambda}\int_{\lambda_m}^{\lambda_M}\sin^2\left(\frac{\delta(\lambda,\xi,\gamma(y))}{2}\right) \times \sin^2\left(2(\Delta + \bar{\alpha} + \alpha(y))\right)\mathrm{d}\lambda + I_{os}, \tag{5}$$

where I_{os} is an offset value which must be considered since all pictures result from a photographic process that usually introduces some light intensity corrections. The average light transmission intensity, within a band j of width $\Delta y_j = y_{jM} - y_{jm}$ taken experimentally from the textures (like those of Fig. 6), can be calculated from equation

$$\langle I\rangle_{band\,j} = \frac{1}{\Delta y_j}\int_{y_{jm}}^{y_{jM}}\langle I\rangle_{\Delta\lambda}(y)\mathrm{d}y. \tag{6}$$

Equations (5) and (6) were used to fit the light transmission profiles presented in Figure 6 and the angular dependence of the light intensity ratio between two successive bands $\langle I\rangle_{band\,j}(\Delta)/\langle I\rangle_{band\,j+1}(\Delta)$, considering I_0, I_{os}, ξ and $\bar{\alpha}$ as free parameters. In these fits we considered $h = 15\,\mu$m, and assumed, as typical values, $\Delta n \sim 0.16$ and $\Delta\lambda = 0.3\,\mu$m. Figures 9 and 10 show two experimental data sets and the best simulated curves obtained by using equations (5) and (6), respectively, considering that the *band j* was the light band at small angles. It can be seen from Figure 9 that the proposed model reasonably describes the periodic modulation observed in the experimental light intensity profile within a *band*, in this case obtained for an angle of 80°. Similar fits could be obtained for other angles. The experimental values of the ratio $\langle I\rangle_{band\,j}(\Delta)/\langle I\rangle_{band\,j+1}(\Delta)$, in Figure 10, clearly show a maximum and a minimum at small and large angles, respectively, which are well fitted by the proposed model. At 45° there is a numerical inversion of the ratio also predicted by the model. At 0° and 90° the *bands j* and $j+1$ have the same light intensity. From this analysis it was possible to estimate for the most significant fitting parameter the values: $\bar{\alpha} \sim 4.6° \pm 0.2°$ and $\xi \sim 1.6° \pm 0.6°$. These values of $\bar{\alpha}$ and ξ are in excellent agreement with those measured from the direct experimental observation presented above.

The proposed model can be used to produce simulated images of the light intensity patterns as a function of angle Δ. In Figure 11 we present patterns for $\Delta = 0°$, 10°, 30°, 45°, 60°, and 80°, in the simple case of a distribution with two values for γ, 90° and 270°, using the values $\bar{\alpha}$ and ξ given above.

As it can be observed, the agreement between the experimental patterns of Figure 6 and those simulated in Figure 11 are quite good.

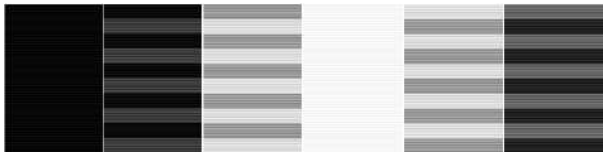

Fig. 11. Simulated optical textures. From left to right, the textures refer to angles Δ of 0°, 10°, 30°, 45°, 60° and 80°, respectively.

Our experimental observations cannot be explained by the original model proposed for the $SmC_?$ phase of DB_8Cl in reference [8]. If, in fact, at the SmC_2-$SmC_?$ transition, the molecules in each sub-layer tilt by an angle β, with respect to the molecular alignment direction in the SmC phase (as shown in Fig. 1), it would not be possible to observe neither the superstructure (bands) nor the short-period modulation (stripes), because the optical director remains the same at the different points of the LC.

The optical model here proposed implies that the bended dimers, introduced in Figure 1, are flexible enough to allow different optical directions in the $SmC_?$ phase, without changing the layer spacing. This makes possible the existence of in-plane and/or out-of-plane molecular distribution of dimers, as illustrated in Figure 12a by dimers A and B, respectively.

In this figure, the upper ends of the dimers have a distribution that describes a closed line in the upper plane of the layer.

This distribution of flexible dimers can be understood in view of the physical theories proposed for the SmC phase, which consider the influence of steric factors and electrostatic interactions between existing static or induced dipoles [12]. In the DB_8Cl compound the molecules have a strong terminal dipole at the cyano group, and another at the chlorine atom connected to the central benzene ring of the molecule's core, therefore resulting in a dipole moment not parallel to the long molecular axis. On the other hand, due to the relative big volume of the chlorine atom with respect to the hydrogen atoms in the molecule, additional steric constraints must contribute to the molecular organization. These aspects must be important to develop a more complex anticlinic-like molecular packing than the one presented in Figure 1 corresponding to the initial model in reference [8]. In fact this dimer may be viewed as a flexible bent-core–like molecule (Figs. 12b and c) and the molecular orientations distribution of dimers illustrated in Figure 12a can be understood as a general distribution of dimers, containing both smectic-C_G and smectic-$C_{B1,B2}$ arrangements [13]. The dimers are represented in Figures 12b and c at particular points to emphasise their possible orientations: all dimer orientations $\mathbf{n}_\gamma$ except those that contain P and Q, correspond to the SmC_G arrangements (Fig. 12b); for those orientations that contain P and Q, it is possible to find, besides the SmC_G structure, certain orientations of dimers where the smectic-C_{B1} and the smectic-C_{B2} structures exist (Fig. 12c). Therefore, the $SmC_?$ phase cannot be strictly associated to one of these banana-like phases.

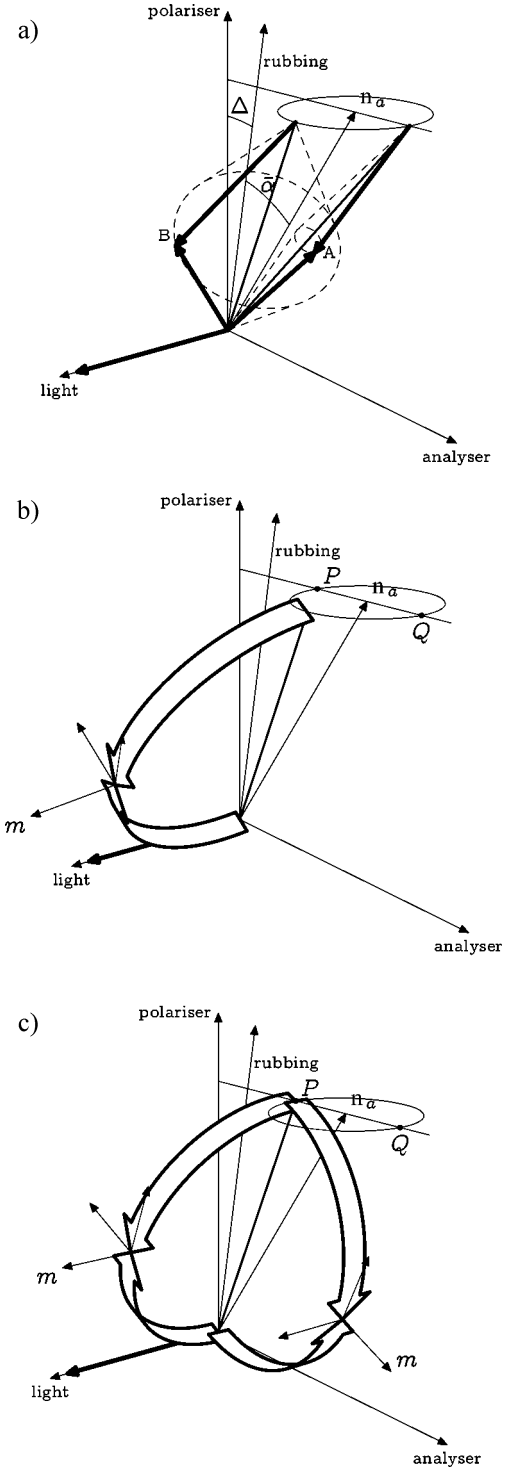

Fig. 12. (a) Schematic representation of the flexible dimers in an in-plane (A) and an out-of-plane (B) optical axis configuration in the $SmC_?$ layer. The bold arrows represent the molecules in a head-to-head configuration; (b) bent-core–like representation of one molecular dimer in a smectic-C_G configuration; (c) bent-core–like representations of a molecular dimer, for the B_1 and B_2 banana-like configurations with the same in-plane optical axis (a similar situation is possible for point Q). m is the dimers's twofold rotation axis [13].

Although the morphological similarity of dimers and bent-core molecules, the former are more flexible because we have two molecules electrostatic bonded to each other and not one rigid molecule. It is also important to notice that the smectic layer's normal is not parallel to the rubbing direction, as it happens in banana-like phases. Both facts seem to be responsible for the many possible dimer orientations in the $SmC_?$ phase, which leads to its peculiar double stripe pattern with lines aligned parallel to the rubbing direction. This pattern was not found on B_1 [14,15], B_2 (SmC_SP_A) [6], B_7 [15] or on the so-called anticlinic-antiferroelectric (SmC_AP_A) B_x phase [16].

The optical results obtained in DB_8Cl show undoubtedly that the $SmC_?$ phase is better aligned and presents a more homogeneously texture than the classical banana phases. The experimental results evidence that the $SmC_?$ phase is more complex than the phases presented by banana-like molecules, resulting from a more general (but not random) orientation of dimers within the smectic layers, whose normal is inclined with respect to the rubbing direction.

Additional experimental work is envisaged in order to clarify the particular details of this mesophase's structure and its polar character.

4 Conclusions

We presented an optical study of the anticlinic-like $SmC_?$ phase of the DB_8Cl compound by polarising microscopy that revealed a peculiar set of band and stripe pattern textures. The most striking fact is the existence of a double periodic modulation of the optical axis of the material, for samples of $25\,\mu$m and $15\,\mu$m thickness. The texture observed is not compatible with the initial model reported in the literature for the $SmC_?$ phase.

The experimental observations here reported were interpreted in terms of a distribution of the principal optical axis, tilted with respect to the rubbing direction of the LC cells, which periodically alternate their tilt angle sign.

The molecular packing in the $SmC_?$ phase was discussed in terms of the physical arguments proposed to explain the nature of the SmC phase and the distribution of the molecular principal optical axis found. We suggest that the molecules in the $SmC_?$ phase are packed as dimers, in a similar way as bent-core molecules. In this phase, the dimers may be oriented in or out of plane, giving rise to a distribution of possible orientations, some of them similar to those observed for classical banana phases, although presenting a more macroscopic optical aligned texture. The results suggest a somehow new and complex banana-like phase. Nevertheless, more experimental results are needed in order to check the molecular packing model here suggested for this phase.

We wish to thank Fundação para a Ciência e Tecnologia (FCT) through projects PRAXIS XXI 3/3.1/MMA/1769/95, POCTI/ISFL/261/516 and Program FEDER/POCTI (Project N°2 - 155/94). The authors also want to thank Prof. Y. Galerne for helpful discussions and L.N. Gonçalves for the help with the software package FEATPOST (`http://www.ctan.org/`) to produce the axis diagrams.

References

1. P.G. de Gennes, J. Prost, *The Physics of Liquid Crystals* 2nd edition (Oxford University Press, 1993).
2. L.M. Blinov, V.G. Chigrinov, *Electro-optic Effects in Liquid Crystal Materials* (Springer Verlag, New York, Inc., 1994) Chapt. 7.
3. A.C. Ribeiro, Y. Galerne, P. Barois, D. Guillon, L. Oswald, Eur. Phys. J. B **11**, 121 (1999).
4. A.C. Ribeiro, H.T. Nguyen, Y. Galerne, D. Guillon, Liq. Cryst. **27**, 27 (2000).
5. C.D. Jones, R.-F. Shao, A.G. Rappaport, J.E. Maclennan, N.A. Clak, E. Körblova, D.M. Walba, Liq. Cryst. **33**, 25 (2006).
6. D.R. Link, G. Natale, R. Shao, J.E. Maclennan, N.A. Clark, E. Körblova, D.M. Walba, Science **278**, 1924 (1997).
7. S. Chandrasekhar, *Liquid Crystals* (Cambridge University Press, Cambridge, 1992); P. Barois, J. Prost, T.C. Lubensky, J. Phys. (Paris) **46**, 391 (1985); J. Prost, P. Barois, J. Chim. Phys. **80**, 65 (1983); H. Nguyen, J. Chim. Phys. **80**, 83 (1983); V. Raja, R. Shashidhar, B. Ratna, G. Heppke, C. Bahr, Phys. Rev. A **37**, 303 (1988).
8. L. Benguigui, F. Hardouin, J. Phys. (Paris) Lett. **45**, 179 (1984).
9. F. Hardouin, Huu Tinh Nguyen, A.M. Levelut, J. Phys. (Paris) Lett. **43**, 779 (1982).
10. A. Carvalho, P.J. Sebastião, H.T. Nguyen, Mol. Cryst. Liq. Cryst. **331**, 89 (1999); A. Carvalho, P.J. Sebastião, A. Ferraz, A.C. Ribeiro, H.T. Nguyen, Eur. Phys. J. E **2**, 351 (2000).
11. M. Born, E. Wolf, *Principles of Optics* (Pergamon Press, UK, 1980).
12. G.W. Gray, J.W.G. Goodby, *Smectic Liquid Crystals* (Leonard Hill, Glasghow and London, 1984).
13. H.R. Brand, P.E. Cladis, H. Pleiner, Eur. Phys. J. B **6**, 347 (1998).
14. J. Szydlowska, J. Mieczkowski, J. Matraszek, D.W. Bruce, E. Gorecka, D. Pociecha, D. Guillon, Phys. Rev. E **67**, 31702 (2003).
15. K. Pelz, W. Weissflog, U. Baumeister, S. Diele, Liq. Cryst. **30**, 1151 (2003).
16. P. Pyc, J. Mieczkowski, D. Pociecha, E. Gorecka, B. Domnio, D. Guillon, J. Mater. Chem. **14**, 2374 (2004).